Copyright © 1996 Elsevier Science Ltd
Paper No. 1248. (quote when citing this article)
Eleventh World Conference on Earthquake Engineering
ISBN: 0 08 042822 3

SYNTHETIC EARTHQUAKE MOTION OF 2-D IRREGULAR GROUND IN NEAR-FIELD

Shojiro KATAOKA and Tatsuo OHMACHI

Interdisciplinary Graduate School of Science and Engineering, Tokyo Institute of Technology
4259 Nagatsuta, Midori-ku, Yokohama 226, JAPAN

ABSTRACT

Since prediction of near-field ground motion is a necessary and important factor to mitigate earthquake damage, quite many studies are devoted to this subject. However, ground irregularity has been rarely taken into account in the prediction. In this study, a new procedure is presented for simulation of earthquake motion of irregular ground in near-field. After dividing a total wave field into free field and scattered field, a discrete wavenumber method is employed for free field excited by faulting, and an FE–BE method is employed for scattered field. Following a simple analysis, seismic motion at Sylmar site during the 1994 Northridge earthquake is simulated by the present procedure. The agreement between the analytical results and the observations is good and shows usefulness of the procedure.

KEYWORDS

near-field; irregular ground; dislocation source; discrete wavenumber method; FE–BE method; earthquake motion; the 1994 Northridge earthquake.

INTRODUCTION

Both the 1994 Northridge earthquake and the 1995 Hyogo-ken Nanbu earthquake took a heavy toll of lives and caused great property damage in the cities near the focal regions. Many lifeline structures such as expressway bridges also collapsed and deferred rescue and rehabilitation.

Most of the collapsed structures are considered to be suffered greater inertia force during the earthquakes than that expected in designing. Thus, in order to mitigate earthquake damage, aseismatic design against near-field ground motion based on dynamic analyses of structures is required. However, if subsurface around a structure under design has much irregularity, it is still difficult to predict strong motion in sufficient accuracy.

Though earthquake motion of irregular ground under incidence of plane waves is studied from various aspects by several methods (e.g., Kawase, 1988; Sánchez-Sesma *et al.*, 1989; Ohori *et al.*, 1992; Mossessian and Dravinski, 1992), few studies discuss that excited by faulting. Vidale and Helmberger(1988) calculated strong motion velocities across the Los Angeles and San Fernando basins during the 1971

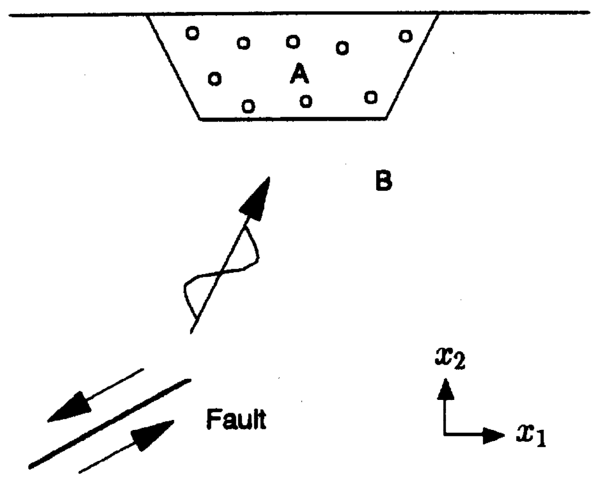

Fig. 1. Outline of an irregular ground and a fault source.

San Fernando earthquake by a finite difference method, using minute basin structure and empirical source model. Yamamoto *et al.*(1992) simulated long period ground motion around the Los Angeles basin during the 1990 Upland earthquake by a boundary element method. Uebayashi *et al.*(1992) investigated characteristics of seismic motion in 3-D sedimentary basins due to a rectangular fault source by the Aki-Larner method.

In this paper, the authors present a new procedure for simulation of earthquake motion of irregular ground excited by faulting. Furthermore, ground motion at Sylmar site during the 1994 Northridge earthquake synthesized by the procedure is compared with observations to examine its practicality.

PROCEDURE FOR SYNTHESIS

From now on, the authors will discuss about 2-D in-plane wave field in frequency domain. Let us analyze response of an irregular ground on which seismic wave generated by faulting is incident, as shown in Fig. 1. In recent years, hybrid techniques that combine the finite element method and the boundary element method(FE–BE method) have been regarded as a valid approach in simulating earthquake motion of an irregular ground (Touhei and Yoshida, 1988; Mossessian and Dravinski, 1992). This is owed to the fact that FE–BE methods make modeling of two different types of ground feasible: finite heterogeneous and infinite homogeneous grounds. The procedure that will be proposed below is based on a conventional FE–BE method; hence, an outline of the FE–BE method and the procedure is presented in this section.

FE–BE Method

If a steady-state wave propagation is assumed and body forces except inertia forces are negligible, equation of motion for 2-D in-plane wave field is specified by

$$(\lambda + \mu)u_{j,ij} + \mu u_{i,jj} + \rho\omega^2 u_i = 0, \tag{1}$$

where u_i denotes x_i-component of the displacement in x_1-x_2 Cartesian coordinate, λ and μ are Lamé's constants, ρ is the mass density, and ω is the angular frequency.

Finite Element Method. By discretizing the region A in Fig. 1 into a set of finite elements, eq.(1) can be written in the following form:

$$[Z]\{u\}_{\mathrm{A}} = \{f\}_{\mathrm{A}}, \tag{2}$$

where $\{u\}$ and $\{f\}$ are the nodal displacement and nodal force vectors, respectively. The subscripts of the vectors denote the region(A or B) which they belong to. If damping effect is considered, the matrix $[Z]$ can be written as

$$[Z] = -\omega^2[M] + i\omega[C] + [K], \tag{3}$$

where $[M]$, $[C]$ and $[K]$ are the global mass, damping and stiffness matrices, respectively, and $i = \sqrt{-1}$.

Boundary Element Method. The boundary integral equation on the boundary Γ of the region B in Fig. 1 is expressed as follows (Niwa *et al.*, 1986):

$$c_{ij}(\boldsymbol{x}_0)u_j(\boldsymbol{x}_0) + \fint_{\Gamma} T_{ij}(\boldsymbol{x},\boldsymbol{x}_0)u_j(\boldsymbol{x})d\Gamma(\boldsymbol{x}) - \int_{\Gamma} U_{ij}(\boldsymbol{x},\boldsymbol{x}_0)t_j(\boldsymbol{x})d\Gamma(\boldsymbol{x}) = \bar{\psi}_i(\boldsymbol{x}_0), \tag{4}$$

where t_i denotes traction on the boundary Γ, U_{ij} the fundamental solution, T_{ij} its traction, $\boldsymbol{x}_0$ and $\boldsymbol{x}$ source and field points, respectively, and c_{ij} a free term depending on the boundary shape at $\boldsymbol{x}_0$.

The term $\bar{\psi}_i$ in eq.(4) represents effects of the incident wave and is derived as follows. Let us write the total wave field in region B as

$$u_i = u_i^{(F)} + u_i^{(S)} \quad \text{and} \quad t_i = t_i^{(F)} + t_i^{(S)}, \tag{5}$$

where $u_i^{(F)}$ and $u_i^{(S)}$ are free field and scattered field, respectively, and $t_i^{(F)}$ and $t_i^{(S)}$ are corresponding tractions. The boundary integral equation for the scattered field can be written as:

$$c_{ij}(\boldsymbol{x}_0)u_j^{(S)}(\boldsymbol{x}_0) + \fint_{\Gamma} T_{ij}(\boldsymbol{x},\boldsymbol{x}_0)u_j^{(S)}(\boldsymbol{x})d\Gamma(\boldsymbol{x}) - \int_{\Gamma} U_{ij}(\boldsymbol{x},\boldsymbol{x}_0)t_j^{(S)}(\boldsymbol{x})d\Gamma(\boldsymbol{x}) = 0. \tag{6}$$

Comparison between eq.(4) and an equation derived by substituting eq.(5) into eq.(6) leads

$$\bar{\psi}_i(\boldsymbol{x}_0) = c_{ij}(\boldsymbol{x}_0)u_j^{(F)}(\boldsymbol{x}_0) + \fint_{\Gamma} T_{ij}(\boldsymbol{x},\boldsymbol{x}_0)u_j^{(F)}(\boldsymbol{x})d\Gamma(\boldsymbol{x}) - \int_{\Gamma} U_{ij}(\boldsymbol{x},\boldsymbol{x}_0)t_j^{(F)}(\boldsymbol{x})d\Gamma(\boldsymbol{x}). \tag{7}$$

By discretizing the boundary Γ into a set of boundary elements, eqs.(4) and (6) can be written in a matrix form as

$$[H]\{u\}_{\mathrm{B}} - [G]\{t\}_{\mathrm{B}} = \{\bar{\psi}\} \quad , \quad \{\bar{\psi}\} = [H]\{u\}^{(F)} - [G]\{t\}^{(F)}, \tag{8}$$

where $\{u\}^{(F)}$ and $\{t\}^{(F)}$ denote nodal displacement and traction vectors of the free field, respectively.

Combining of Matrix Equations. Continuity and equilibrium conditions along the boundary between region A and B require that

$$\{u\}_{\mathrm{A}} = \{u\}_{\mathrm{B}} \quad , \quad \{f\}_{\mathrm{A}} = -[D]\{t\}_{\mathrm{B}}. \tag{9}$$

The distribution matrix $[D]$ depends on the type of interpolation functions (Brebbia *et al.*, 1984). The FE–BE analysis is carried out by solving eqs.(2), (8) and (9) simultaneously.

Incorporating the Discrete Wavenumber Method

The vectors $\{u\}^{(F)}$ and $\{t\}^{(F)}$ are easily obtained if plane waves are incident on. Here, the authors adopted the discrete wavenumber method (Bouchon and Aki, 1977) to calculation of these vectors for

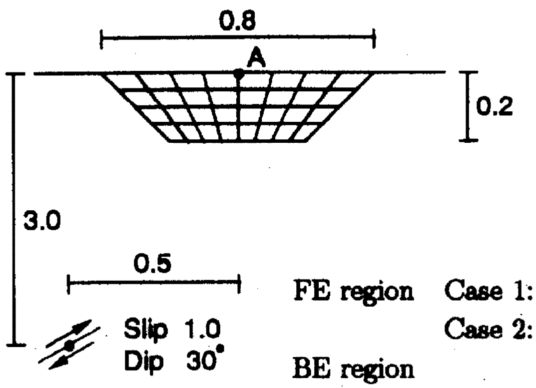

Fig. 2. Analytical model.

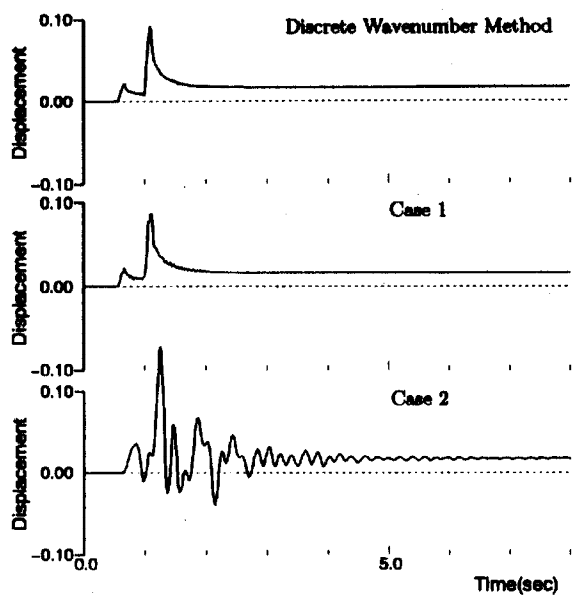

Fig. 3. Comparison of horizontal synthetic motions at point A.

wave field excited by faulting. In the general discrete wavenumber representation, a complex angular frequency $\hat{\omega}$ ($= \omega - i\omega_I, \omega_I > 0$) is applied to computation to avoid Rayleigh poles. Consequently, the vectors are derived as functions of $\hat{\omega}$; this requires the FE–BE analysis should be carried out in terms of $\hat{\omega}$. As a result, a response in time domain $u(t)$ is finally derived by inverse Fourier transform of $U(\hat{\omega})$, which represents the solution of the simultaneous equations (2), (8) and (9) , i.e.,

$$u(t) = \exp(\omega_I t) \int_{-\infty}^{\infty} U(\hat{\omega}) S(\hat{\omega}) \exp(i\omega t) d\omega, \tag{10}$$

where $S(\hat{\omega})$ denotes a Fourier transform of a source time function.

As stated above, the present procedure employs two methods: the discrete wavenumber method for free field and the FE–BE method for scattered field.

CHECK OF VALIDITY

Simulations of a simple problem are carried out for two cases by the present procedure. Fig. 2 shows the analytical model consisting of an irregular ground and a seismic source. The source is a point dislocation represented by a double coupe force. Material properties of FE and BE regions are same

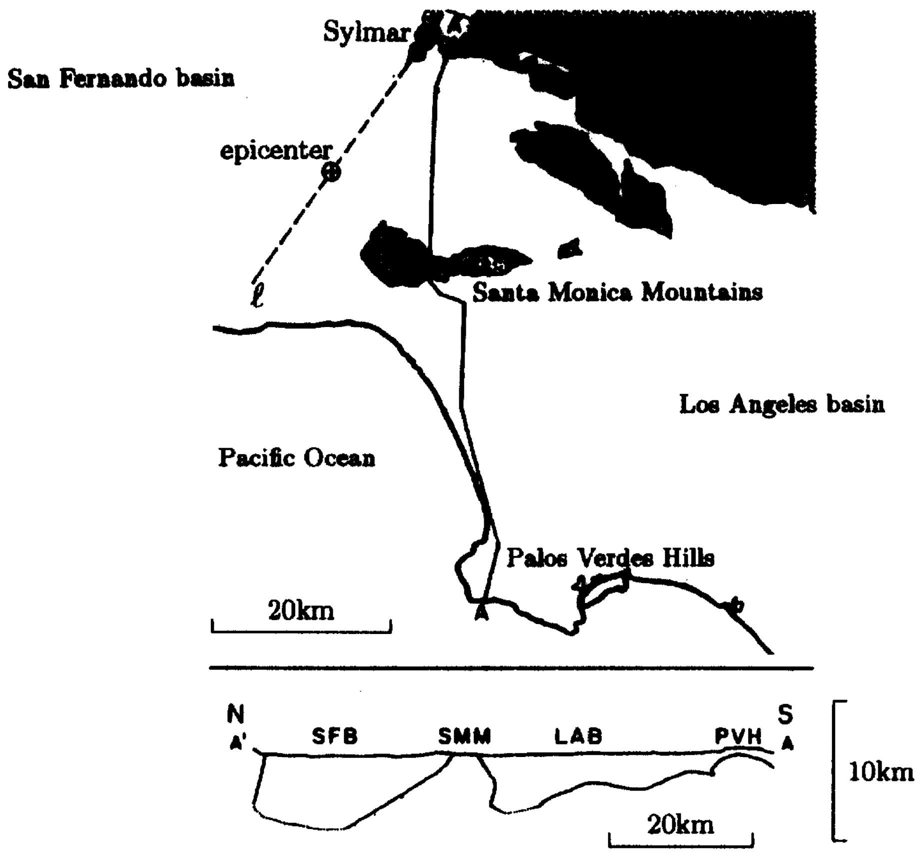

Fig. 4. Map and cross-section of the San Fernando region (Vidale and Helmberger, 1988). Cross-hatched areas show outcrop of the bedrock. The profile along A–A' is shown below.

in case 1; they are different in case 2. The properties are shown in Fig. 2, where V_s and ν denote S-wave velocity and Poisson's ratio, respectively. In case 2, slight internal damping is considered as Rayleigh damping. Since the ground model in case 1 is identical to homogeneous half space, the discrete wavenumber method is applied to the same analysis. A ramp function having rise time of 0.1 sec is used as the source time function.

As shown in Fig. 3, results from case 1 and the discrete wavenumber method agrees well and accuracy of the present procedure is sufficient. The synthetic in case 2 shows large amplitude and long duration of earthquake motion caused by geometrical and material irregularities.

SIMULATION OF THE NORTHRIDGE EARTHQUAKE

A simulation of an actual earthquake is here presented to demonstrate practicality of the procedure for prediction of near-field ground motion.

During the 1994 Northridge earthquake, the accelerograph in the parking lot of the Sylmar County Hospital, which is 15km distant from the epicenter, recorded a peak horizontal acceleration(NS component) of 827cm/s^2 (Darragh *et al.*, 1994). Fig. 4 shows the map of the San Fernando region including locations of the epicenter and Sylmar. The authors thought it possible to treat the wave field as 2-D in-plane one along the broken line ℓ in Fig. 4 , for the following reasons: 1) the azimuth of Sylmar from the epicenter is N35E, and 2) the fault is reverse with the strike directing N122E (Wald and Heaton, 1994).

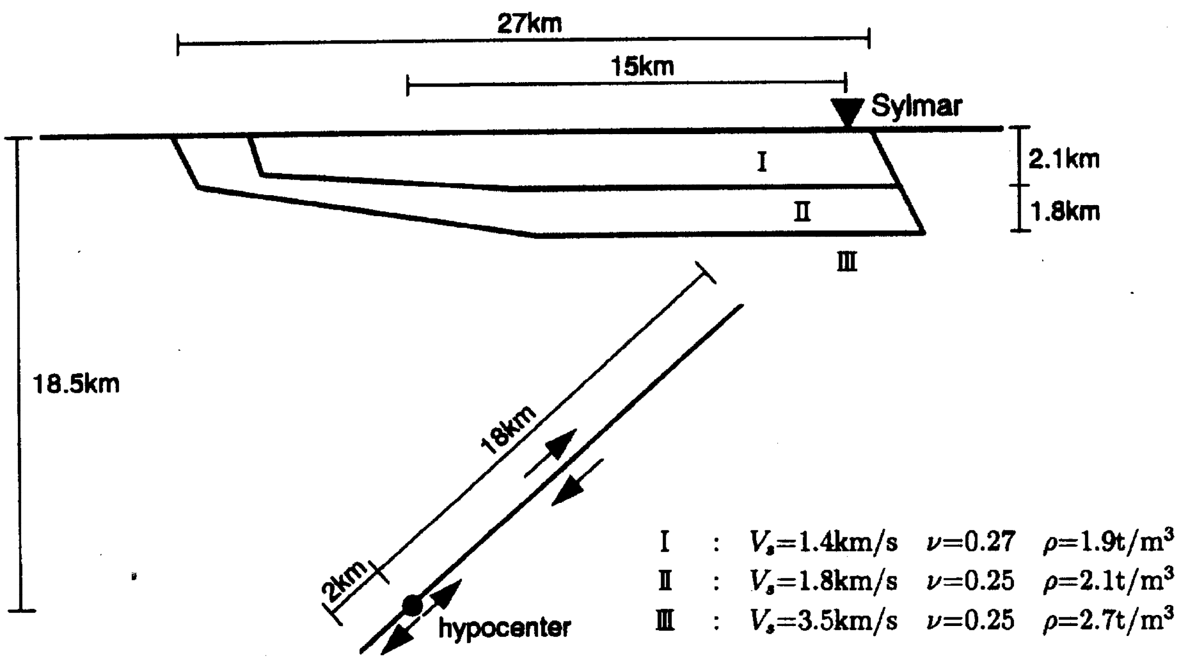

Fig. 5. Analytical model of the San Fernando basin and the fault of the 1994 Northridge earthquake.

Table 1. Fault model parameters determined by Wald and Heaton (1994).

date	January 17, 1994
origin time	12:30 55.2 GMT
focal depth	18.5km
strike	122°
dip	42°
effective fault width	20km
fault depth range	6.0–20.0km
average slip	1.2m
rupture velocity	2.8km/sec
rise time	0.6–1.2sec

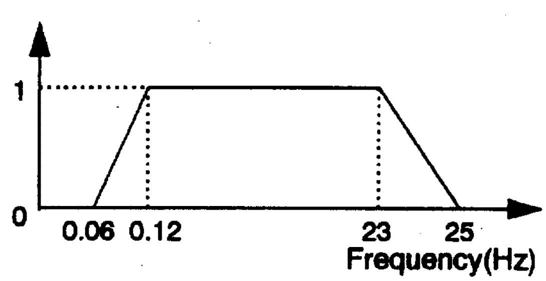

Fig. 6. Band pass filter applied to the observations and synthetics.

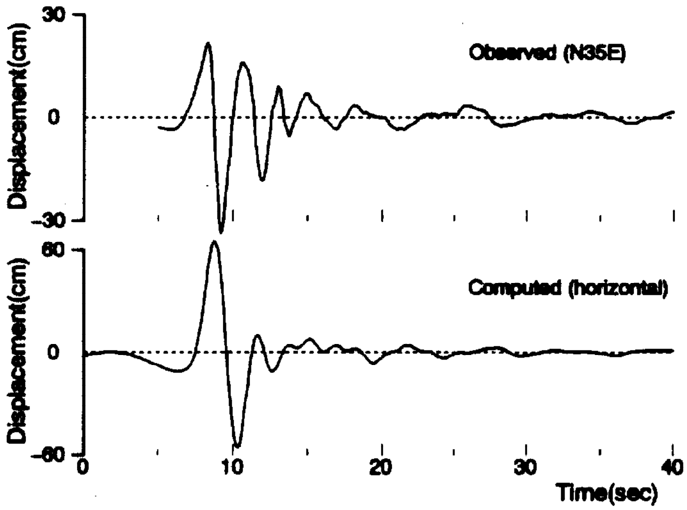

Fig. 7. Comparison of the computed horizontal motion with N35E component of the observed displacement.

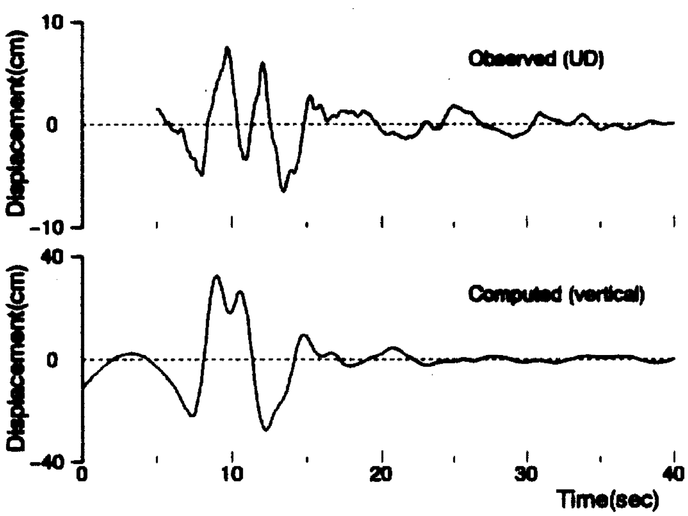

Fig. 8. Comparison of the computed vertical motion with UD component of the observed displacement.

Modeling of the Structure and Fault

Vidale and Helmberger (1988) simulated the 1971 San Fernando earthquake in the A'–A profile in Fig. 4. Since the structure under ℓ is not known, the authors modeled it as shown in Fig. 5, referring to Fig. 4 and structural cross-section of the A'–A profile (Vidale and Helmberger, 1988). In Fig. 5, the regions I and II are discretized by finite elements; the boundary of the region III is discretized by boundary elements. All the elements are linear isoparametric ones. After the study of Vidale and Helmberger (1988), a seismic attenuation Q of about 25 is considered in the regions I and II as Rayleigh damping.

Table 1 shows the fault model parameters determined from the inversion of strong motion recordings and distribution of aftershocks(Wald and Heaton, 1994), which is used in the calculation of free field by the discrete wavenumber method. Though the rise time is estimated to vary between 0.6 and 1.2 sec within the fault plane, it is set to constant at 0.9 sec.

Comparison of Synthetics with Observations

Since the recorded motions were filtered (Darragh *et al.*, 1994), the same filter shown in Fig. 6 is applied to synthetics. Figs. 7 and 8 compare the filtered synthetics and observations: the computed horizontal motion and the N35E component of observed displacement are compared in Fig. 7; the vertical components of the computed and observed motions are compared in Fig. 8. The origin time is estimated at 12:30 55.2 GMT as shown in Table 1 and the trigger time of the observations is 12:31 00.2 UTC. The initial time of the synthetics corresponds to the origin time; thus the observations begin just at 5 sec. As a whole, the agreement between the synthetics and observations is good despite the rough modeling. However, displacements are different in amplitude; that is, the peak values of horizontal and vertical synthetic motions are about 2 and 4 times as large as those of observations, respectively. This implies that three-dimensional effects and nonlinearity of soils should be considered.

CONCLUSIONS

A new procedure for synthesis of near-field earthquake motion of irregular ground is proposed. Incorporating a discrete wavenumber method into an FE–BE method makes it possible to synthesize the motion. The ground motion at Sylmar site during the 1994 Northridge earthquake has been well simulated by the procedure. Extension of the procedure to three-dimensional space is possible without difficulty, and necessary to temper the difference arose in this study.

REFERENCES

Bouchon, M. and K. Aki (1977). Discrete wave-number representation of seismic-source wave fields, *Bull. Seism. Soc. Am.*, **67**, 259–277.

Brebbia, C.A., J.C. Tells and L.C. Wrobel (1984). *Boundary Element Techniques–Theory and Applications in Engineering*, Springer-Verlag, Berlin.

Darragh, R., T. Cao, C. Cramer, M. Huang and A. Shakal (1994). Processed CSMIP strong-motion records from the Northridge, California earthquake of January 17 1994, Release No.1.

Kawase, H. (1988). Time-domain response of a semi-circular canyon for incident SV, P, and Rayleigh waves calculated by the discrete wavenumber boundary element method. *Bull. Seism. Soc. Am.*, **78**, 1415–1437.

Mossessian, T.K. and M. Dravinski (1992). A hybrid approach for scattering of elastic waves by three-dimensional irregularities of arbitrary shape. *J. Phis. Earth*, **40**, 241–261.

Niwa, Y., S. Hirose and M. Kitahara (1986). Application of the boundary integral equation (BIE) method to transient response analysis of inclusions in a half-space. *Wave Motion*, **8**, 77–91.

Ohori, M., K. Koketsu and T. Minami (1992). Seismic responses of three-dimensionally sediment-filled valleys due to incident plane waves. *J. Phis. Earth*, **40**, 209–222.

Sánchez-Sesma, F.J., L.E. Pérez-Rocha and S. Chávez-Pérez (1989). Diffraction of elastic waves by three-dimensional surface irregularities. Part II. *Bull. Seism. Soc. Am.*, **79**, 101–112.

Touhei, T. and N. Yoshida (1988). A coupled boundary and finite element method for the time marching analysis. *Proc. 9th World Conf. Earthq. Eng.*, **2**, 623–628.

Uebayashi, H., M. Horike and Y. Takeuchi (1992). Seismic motion in a three-dimensional arbitrarily-shaped sedimentary basin, due to a rectangular dislocation source. *J. Phis. Earth*, **40**, 223–240.

Vidale, J.E. and D.V. Helmberger (1988). Elastic finite-difference modeling of the 1971 San Fernando, California earthquake. *Bull. Seism. Soc. Am.*, **78**, 122–141.

Wald, J.D. and T.H. Heaton (1994). A dislocation model of the 1994 Northridge, California, earthquake determined from strong ground motions, *U.S.G.S. Open-File Report*, 94–278.

Yamamoto, S., Y. Hisada and S. Tani (1992). Simulations of long period strong ground motions during the 1990 Upland earthquake, California. *Proc. 10th World Conf. Earthq. Eng.*, 1127–1132.